

Supporting Information

Super-reductive mesoporous phosphomolybdate with high crystallinity and its excellent performance for Li-ion battery application

Hamid Ilbeygi^a, Sungho Kim^{b,c}, In Young Kim^{b,d*}, Stalin Joseph^b, Min Gyu Kim^e and Ajayan Vinu^b**

^aDr. Hamid Ilbeygi

Future Industries Institute (FII), University of South Australia, Mawson Lakes, SA 5095, Australia

^bDr. Sungho Kim, Prof. In Young Kim, Dr. Stalin Joseph, Prof. Ajayan Vinu

Global Innovative Center for Advanced Nanomaterials, College of Engineering, Science and Environment, The University of Newcastle, Callaghan, NSW 2308, Australia

^cDr. Sungho Kim

Central Research Facilities, Gwangju Institute of Science and Technology, Gwangju 61005, Republic of Korea

^dProf. In Young Kim

Department of Chemistry, College of Natural Sciences, Chonnam National University, Gwangju 61186, Republic of Korea

^eDr. Min Gyu Kim

Pohang Accelerator Laboratory, Pohang University of Science and Technology, Pohang 37673, Republic of Korea

E-mail: ajayan.vinu@newcastle.edu.au

E-mail: hamid.ilbeygi@unisa.edu.au

E-mail: inyoung.kim@jnu.ac.kr

Figure S1. The low-angle XRD pattern of mPMA.

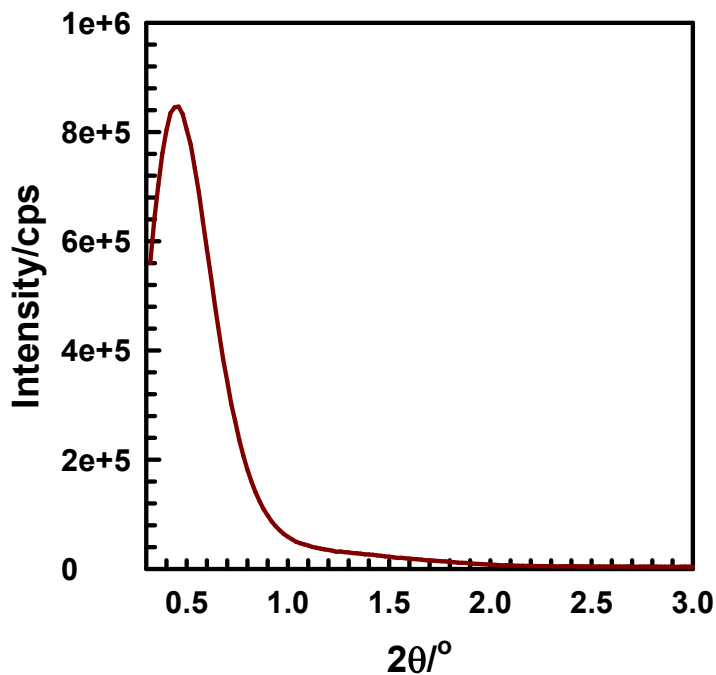


Figure S2. The pore size distribution curve of mPMA.

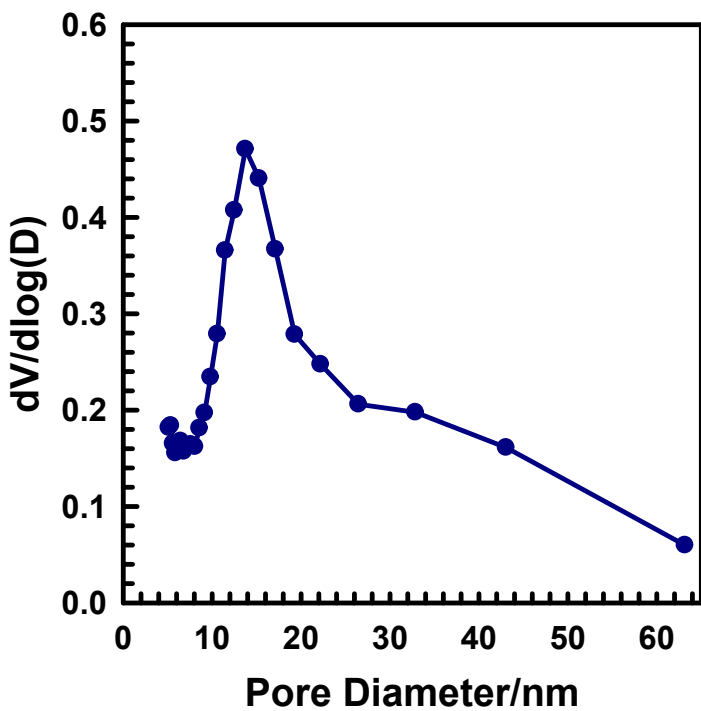
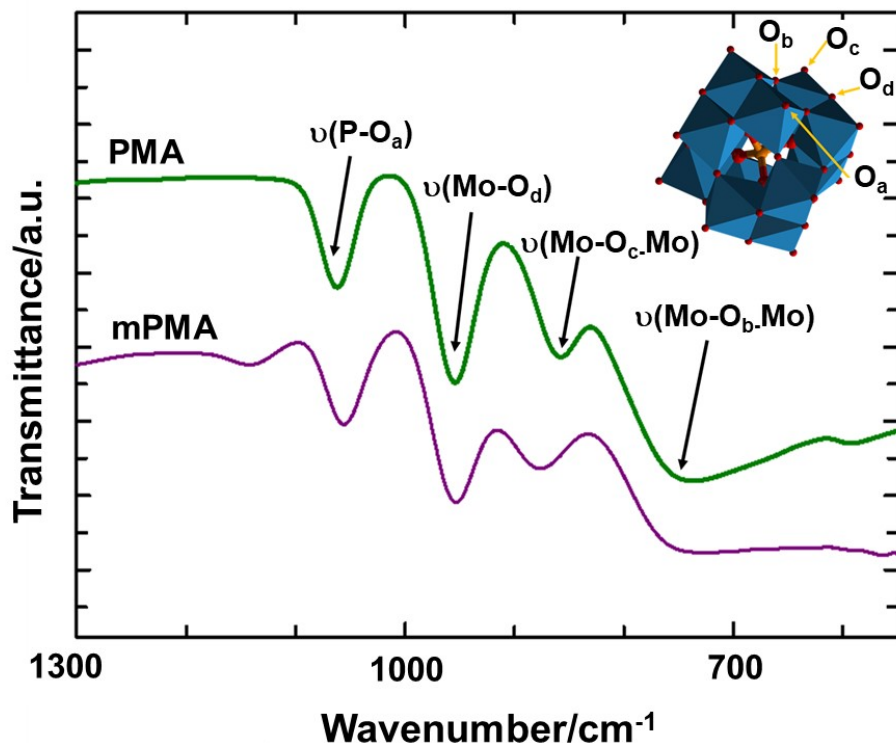


Figure S3. FTIR spectroscopy of mPMA and bulk PMA.



The chemical bonding of mPMA was investigated by Fourier transform-infrared (FT-IR) spectroscopy. The bulk PMA shows the characteristic absorption bands at ~ 770 , ~ 859 , ~ 955 and $\sim 1061\text{ cm}^{-1}$, which can be assigned to the stretching modes of edge-sharing Mo-O_b-Mo and corner-sharing Mo-O_c-Mo in MoO₆ octahedra, terminal Mo-O_d bonds and P-O_a bonds in PO₄ tetrahedron respectively. The absorption peaks at $\sim 1050\text{ cm}^{-1}$ and $\sim 593\text{ cm}^{-1}$ are assigned to the P-O stretching mode of distorted PO₄ central unit and the stretching vibration mode of O-P-O bonds, respectively. In addition mPMA, shows a slight band below 1200 cm⁻¹ compared to bulk PMA, this also demonstrates the PMA clusteres are trapped within the mesochanneled formed by keggin anion and potassium ion but they ave retained their inherent structure. The mPMA

samples exhibit a shift of the Mo-O_d and Mo-O_b-Mo absorption bands to lower wavenumber region, confirming strongly bonded Keggin anions within the mesostructure.

Figure S4. P 2p high resolution XPS spectra of mPMA and bulk PMA.

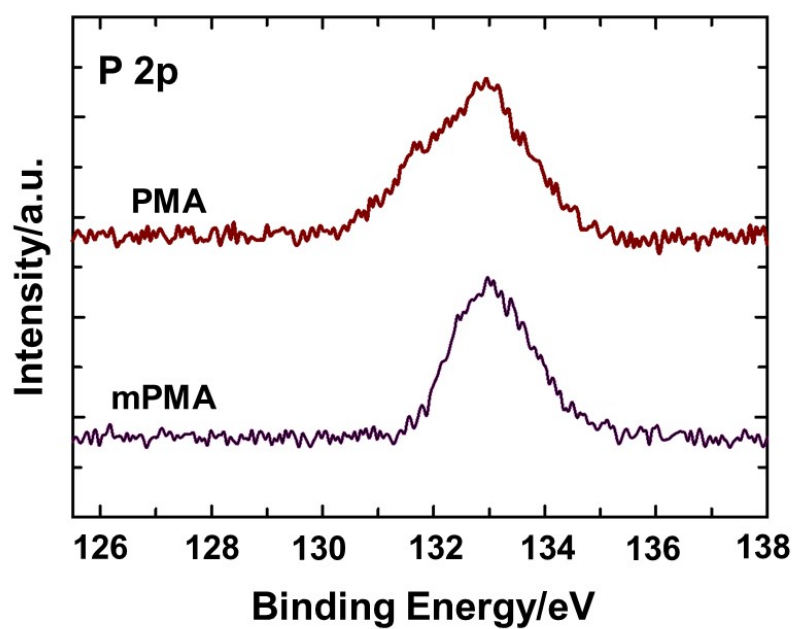


Figure S5. Thermal gravimetric analysis for mPMA and bulk PMA.

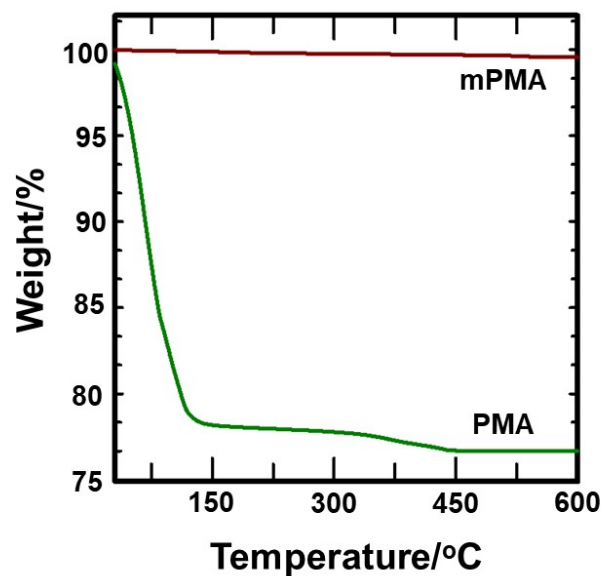


Figure S6. galvanostatic charge-discharge potential profiles at different current densities for the mPMA anode.

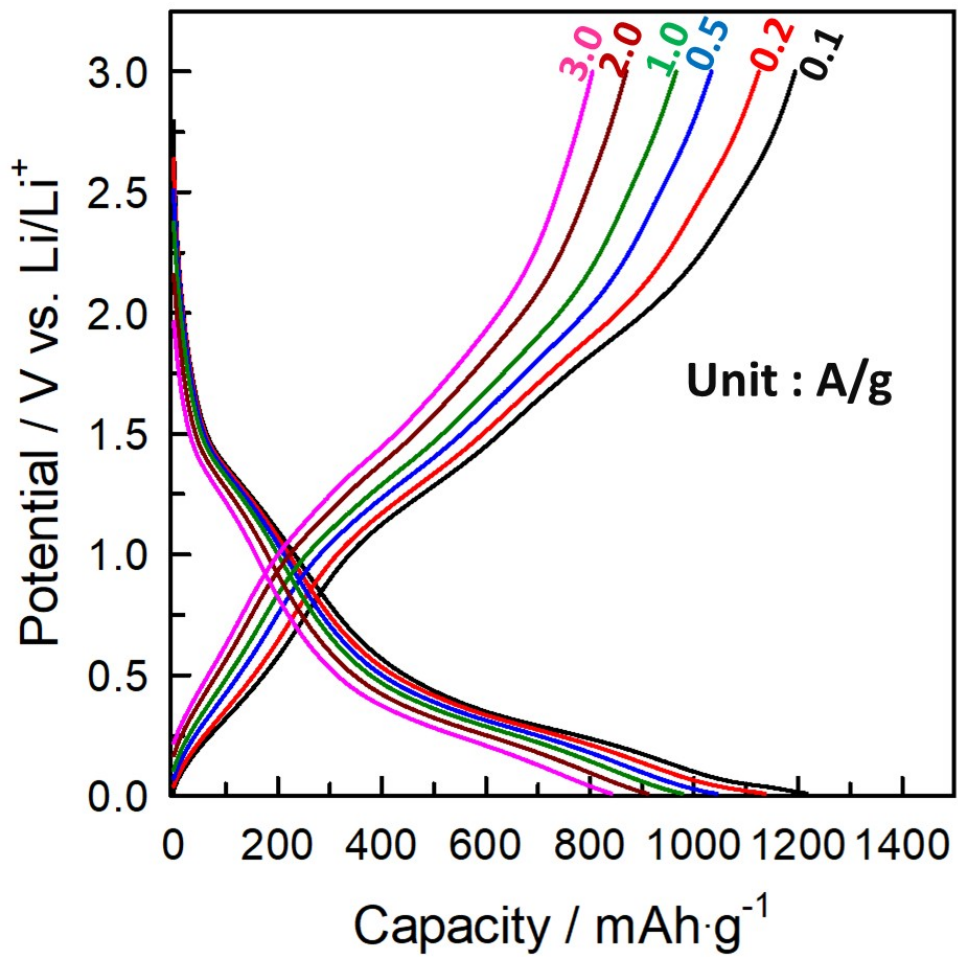


Figure S7. *Ex situ* XRD of mPMA electrode at four different voltages in the initial cycling, where the electrode discharges until 1.5 V (red) and 0.01 V (green) and then charges to ~1.5 V (blue) and 3.0 V (pink). Triangles represent the Bragg reflections corresponding to mPMA structure.

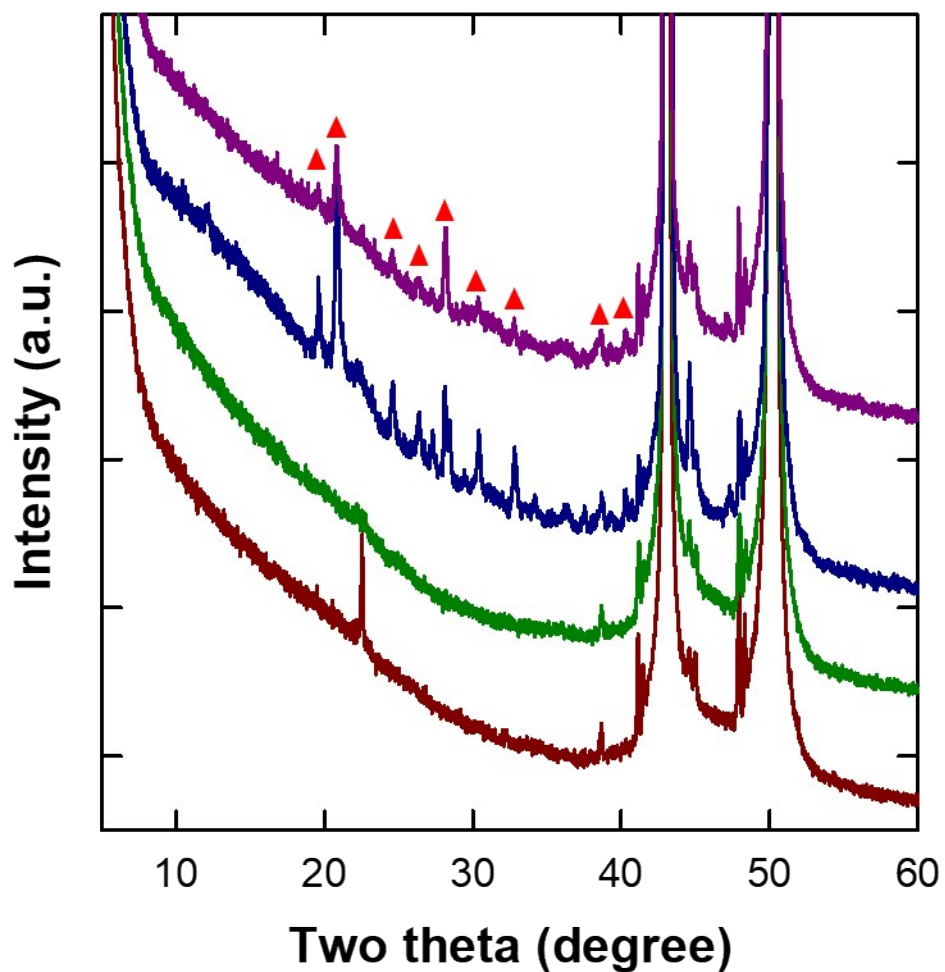


Figure S8. (a) Potential profiles, (b) charge-discharge capacities with Coulombic efficiency at 0.2 Ag^{-1} and (c) rate capability under different current densities of PMA

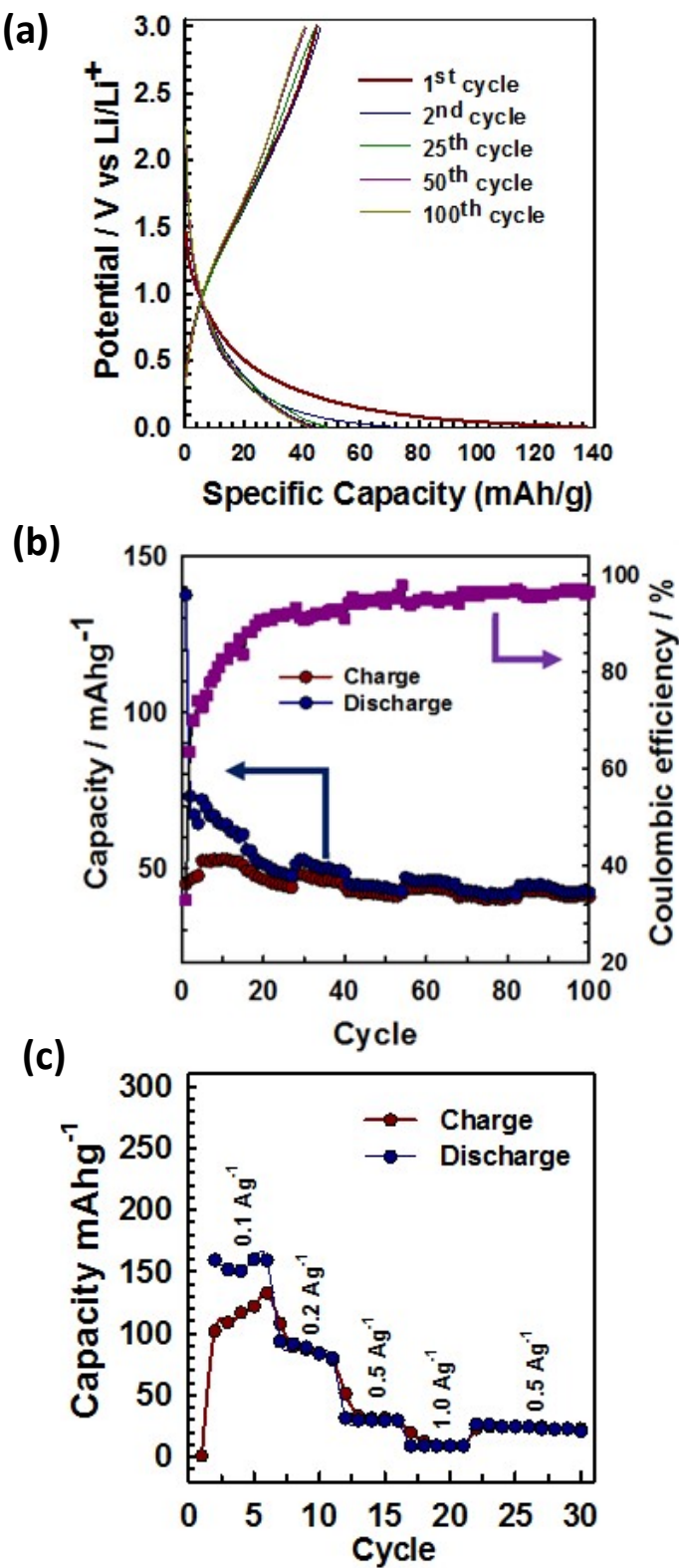


Figure S9. GITT curves of **mPMA** (a) first discharging profile, (b) charging profile and its corresponding estimated Li^+ diffusion coefficients (c) and (d).

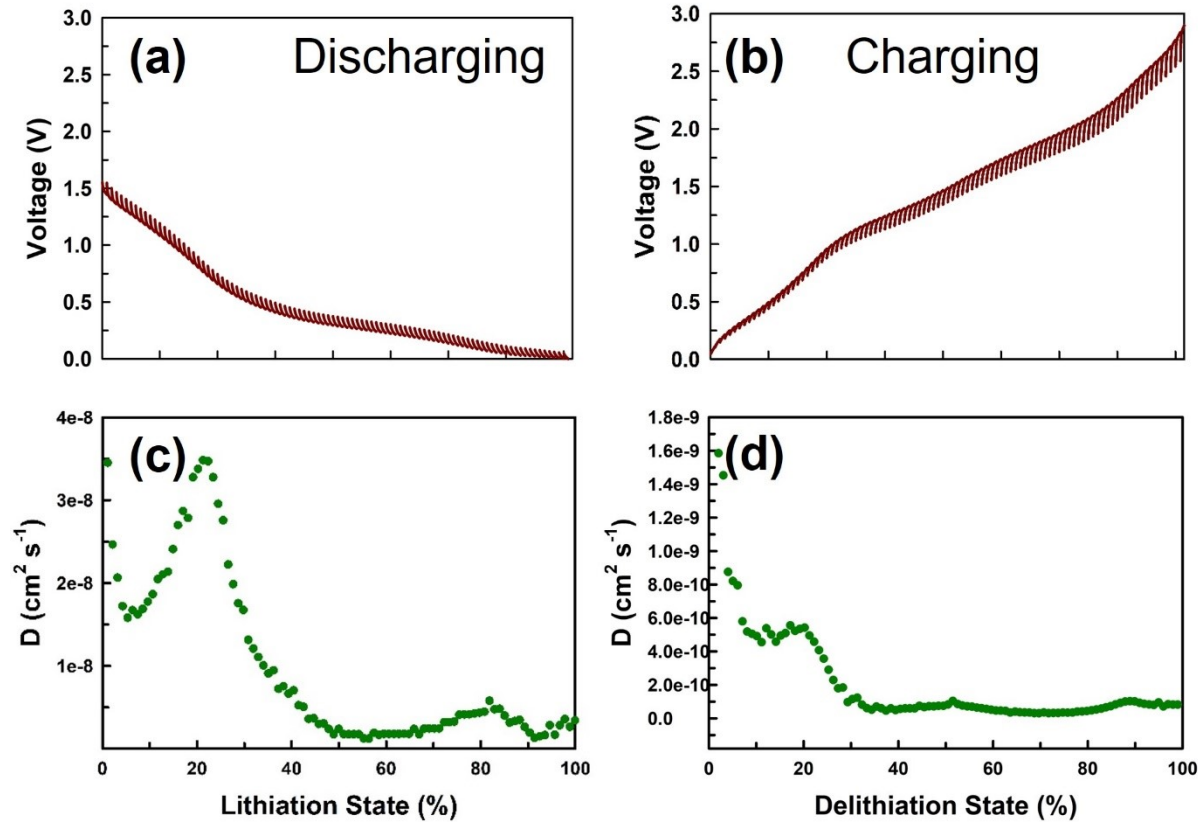


Table S1. Comparison of electrode performances of molybdenum oxide-based materials for LIBs.

Material	Current density	Voltage window (V)	Discharge capacity (mA h g ⁻¹)	Ref.
MoO ₂ /C	200 mA g ⁻¹	0.005-3.0	810	1
MoOC/MoO ₂ -NCNW	500 mA g ⁻¹	0.05-3.0	860	2
Hollow MoO ₂ /C	1000 mA g ⁻¹	0.01-3.0	810	3
MoO _{3-x} nanowire	200 mA g ⁻¹	0.1-3.5	580	4
Mixed molybdenum Oxides	200 mA g ⁻¹	0.005-3.0	930.6	5
Vanadium oxide/molybdenum oxide hybrid	200 mA g ⁻¹	0.01-3.0	1380	6
Molybdenum oxide Nanobelt	500 mA g ⁻¹	0.01-3.0	291	7
Mesoporous PMA	500 mA g⁻¹	0.01-3.0	1517	This work

Table S2. Comparison of performances of high performing and durable electrode materials for LIBs.

Material	Current density	Voltage window (V)	Discharge capacity (mA h g ⁻¹)	No. cycles	Ref.
Fe ₂ O ₃ /TiO ₂	0.5 A g ⁻¹	0.01-1.0	1056	1000	8
Hollow SnO ₂ -C hybrid nanoparticles	0.5 A g ⁻¹	0.01-3.0	995	500	9
HfO ₂ coated SnO ₂ /MXene	0.5 A g ⁻¹	0.01-3.0	843	50	10
Carbon-Encapsulated Nb ₂ O ₅ Nanocrystals	1.0 A g ⁻¹	0.01-3.0	150	1000	11
NiS _x @C yolk-shell	1.0 A g ⁻¹	0.01-3.0	460	2000	12
CuGeO ₃ ultrathin nanosheets/graphene	1.0 A g ⁻¹	0.01-3.0	693	500	13
SnO ₂ @MOF	1.0 A g ⁻¹	0.01-3.0	450	1000	14
H-TiO ₂ @SnS ₂ @PPy	2.0 A g ⁻¹	0.01-3.0	508	2000	15
Graphene encapsulated ZnO-Mn-C hollow microspheres	5.0 A g ⁻¹	0.01-3.0	422	1600	16
Mesoporous PMA	0.5 Ag⁻¹	0.01-3.0	1517	200	This work
	5.0 A g⁻¹	0.01-3.0	521	500	
Al@TiO ₂ yolk-shell	10 C ⁺	0.06-2.0	661	500	17
Three-dimensional holey-graphene/nobia	10 C [*]	1.1-3.0	125	10000	18

[†] 1 C=1410 mA g⁻¹

^{*} 10 C= 22 mA cm⁻²

References for Supplementary Information

- [1] Y. Yao, Z. Chen, R. Yu, Q. Chen, J. Zhu, X. Hong, L. Zhou, J. Wu, L. Mai, ACS App. Mat. & Inter. 2020, **12**, 40648- 40654.
- [2] J. Cuan, Y. Zhou, J. Zhang, T. Zhou, G. Liang, S. Li, X. Yu, W.K. Pang, Z. Guo, ACS Nano, 2019, **13**, 11665- 11675.
- [3] W. Tian, H. Hu, Y. Wang, P. Li, J. Liu, J. Liu, X. Wang, X. Xu, Z. Li, Q. Zhao, H. Ning, W. Wu, M. Wu, ACS Nano, 2018, **12**, 1990 - 2000.
- [4] P. Meduri, E. Clark, J.H. Kim, E. Dayalan, G.U. Sumanasekera, M.K. Sunkara, Nano Lett. 2012, **12**, 1784- 1788.
- [5] D. Wu, R. Shen, R. Yang, W. Ji, M. Jiang, W. Ding, L. Peng, Sci. Rep. 2017, **7**, 44697.
- [6] C. Jo, W.-G. Lim, A.H. Dao, S. Kim, S. Kim, S. Yoon, J. Lee, J. Mater. Chem. A. 2017, **5** 24782.
- [7] C. Wu, H. Xie, D. Li, D. Liu, S. Ding, S. Tao, H. Chen, Q. Liu, S. Chen, W. Chu, B. Zhang, L. Song, The J. Phys. Chem. Lett. 2018, **9**, 817-824.
- [8] D. Qu, Z. Sun, S. Gan, L. Gao, Z. Song, H. Kong, J. Xu, X. Dong, L. Niu, ChemElectroChem, 2020, **7**, 4963-4970.
- [9] L. Zhou, J. Zhang, Y. Wu, W. Wang, H. Ming, Q. Sun, L. Wang, J. Ming, H.N. Alshareef, Adv. Energy Mater. 2019, **0**, 1902194.
- [10] B. Ahmed, D.H. Anjum, Y. Gogotsi, H.N. Alshareef, Nano Energy, 2017, **34**, 249-256.
- [11] X. Han, P.A. Russo, N. Goubard-Bretesché, S. Patanè, S. Santangelo, R. Zhang, N. Pinna, Adv. Energy Mater. 2019, **0**, 1902813.
- [12] Q. Li, L. Li, P. Wu, N. Xu, L. Wang, M. Li, A. Dai, K. Amine, L. Mai, J. Lu, Adv. Energy Mater. 2019, **0**, 1901153.
- [13] Y. Liu, T. Zhou, Y. Zheng, Z. He, C. Xiao, W.K. Pang, W. Tong, Y. Zou, B. Pan, Z. Guo, Y. Xie, ACS Nano, 2017, **11**, 8519- 8526.
- [14] C. Gao, Z. Jiang, P. Wang, L.R. Jensen, Y. Zhang, Y. Yue, Nano Energy, 2020, **74**, 104868.
- [15] L. Wu, J. Zheng, L. Wang, X. Xiong, Y. Shao, G. Wang, J.-H. Wang, S. Zhong, M. Wu, Angew. Chem. Int. Ed. 2019, **58**, 811- 815.
- [16] Q. Xie, P. Liu, D. Zeng, W. Xu, L. Wang, Z.-Z. Zhu, L. Mai, D.-L. Peng, Adv. Func. Mater. 2018, **28**, 1707433.

[17] S. Li, J. Niu, Y.C. Zhao, K.P. So, C. Wang, C.A. Wang, J. Li, Nat. Comm. 2015, 6, 7872.

[18] H. Sun, L. Mei, J. Liang, Z. Zhao, C. Lee, H. Fei, M. Ding, J. Lau, M. Li, C. Wang, X. Xu, G. Hao, B. Papandrea, I. Shakir, B. Dunn, Y. Huang, X. Duan, Science, 2017, 356, 599.